Polymer 52 (2011) 2600–2608

Contents lists available at ScienceDirect

Polymer

journal homepage: www.elsevier.com/locate/polymer

Substituent-induced delocalization effects on hydrogen-bonding interaction in poly(*N*-phenyl methacrylamide) derivatives

Shiao-Wei Kuo [a,*], Chien-Ting Lin [b], Jem-Kun Chen [b], Fu-Hsiang Ko [b], Feng-Chih Chang [b], Kwang-Un Jeong [c]

[a] Department of Materials and Optoelectronic Science, Center for Nanoscience and Nanotechnology, National Sun Yat-Sen University, Kaohsiung 804, Taiwan, ROC
[b] Institute of Applied Chemistry, National Chiao Tung University, Hsin Chu 300, Taiwan, ROC
[c] Department of Polymer-Nano Science and Technology, Chonbuk National University, Jeonju 561-756, South Korea

ARTICLE INFO

Article history:
Received 10 December 2010
Received in revised form
25 March 2011
Accepted 10 April 2011
Available online 15 April 2011

Keywords:
Polymer blend
Hydrogen bonding
Miscibility

ABSTRACT

Within small molecules, the hydrogen-bonding behaviors affected by delocalization have been studied thoroughly, but rare publication in macromolecules. Therefore, three poly(*N*-phenyl methacrylamide)s, poly(*N*-phenyl methacrylamide) (PNPAA), poly(*N*-4-methoxyphenyl methacrylamide) (PMPMA) and poly(*N*-4-bromophenyl methacrylamide) (PBPMA), with different inductive substitution at *para* position of benzene ring are prepared to investigate the substituent-induced delocalization effects on the hydrogen-bonding interaction behaviors. In this study, the variable-temperature FTIR spectrum is used as tool to study the self- and inter-association hydrogen-bonding interaction. FTIR analyses could provide evidences that there is relatively stronger inter-associative hydrogen bonding in poly(*N*-4-bromophenyl methacrylamide)/P4VP blends. High resolution ^{13}C CP/MAS solid-state NMR analyses indicate that the spin-lattice relaxation time ($T_1\rho^H$) in all PBPMA blends are homogeneous on the scale at which spin-diffusion occurs within the time $T_1\rho^H$, also due to the enhancement by substituent inductive delocalization.

1. Introduction

Specific interactions between various polymers concerning with different structures have been intensively reported, especially for those in hydrogen-bonding blend systems such as homopolymer/homopolymer [1–7], homopolymer/copolymers [7–19], and ternary blends [20–23]. Most studies have concentrated on the understanding of structural effects on self- or inter-associative hydrogen bonding in polymer blends. The accessibility of functional groups in hydrogen-bonded polymer blends has significantly affected the intramolecular screening effects which are a direct consequence of the chain connectivity [24–26]. In addition, the acidity or basicity of hydrogen-bond donor, steric hinderance, and temperature would also affect the inter-association hydrogen bonding in polymer blend system [2,27]. For blends of nonpolar polymers [28], the mixing process is thermodynamic unfavorable because of decreasing the combinational entropy of mixing as blending two or more polymers. However, the miscibility can be enhanced by introducing specific interaction, especially hydrogen bonding, to decrease the van Laar type energy of interaction characterized by a Flory–Huggins interaction parameter.

There are some factors which could affect the strength of hydrogen bonding, including the nature of hydrogen donors and acceptors, temperature, solvent, and so on [29,30]. Particularly, in the nature of hydrogen-bond donors and acceptors, the resonance of electrons between donors and acceptors plays an important role in affecting the strength of hydrogen bonding. This resonance effect can redistribute the electron density on the hydrogen donors and acceptors by the driving force that having the conformation of structure to reach a most stable state. In addition, it can affect the basicity of the acceptors, further influence the strength of hydrogen bonding. Therefore, the strength of hydrogen bonding between the chemical structure which containing the resonance effect, or not, may exist some difference. In the small molecules field, the resonance effect on the intra-associative hydrogen bonding could be analyzed by the atoms in molecules (AIM) and density functional theory (DFT) [31,32]. The donor-acceptor distance of *cis*-enol tautomer of malonaldehyde was reduced by the π-electron delocalization between the donor and acceptor atoms to enhance the strength of malonaldehyde's intra-association, because the π-electron delocalization would change the electron-cloud distribution both on donors and acceptors, inducing the charge

* Corresponding author. Tel./fax: +886 7 5254099.
E-mail address: kuosw@faculty.nsysu.edu.tw (S.-W. Kuo).

0032-3861/$ – see front matter © 2011 Elsevier Ltd. All rights reserved.
doi:10.1016/j.polymer.2011.04.016

formation and thus enhancing the strength of self-association. These theories may be difficult to apply in polymers because of chain connectivity that can complicate polymer hydrogen-bonding interaction, but the resonance effects cannot be ignored.

The resonance effect on hydrogen-bonding behaviors in a binary polymer blend has been disclosed in our previous publication [33]. The electron-cloud distribution of (O═)C–N–H group in poly(-*N*-phenyl methacrylamide) (PNPAA) is almost a planar, and the aromatic ring in PNPAA can make the carbonyl group electron-deficient through delocalization via the lone-paired electrons on nitrogen atom, resembling an electron-withdrawing group. Furthermore, when a pyridine group in P4VP forms a hydrogen bond with the N–H group in PNPAA, a planar delocalization, constructed by the aromatic-π system of pyridine in P4VP, the aromatic-π system and the carbonyl-π system of amide group in PNPAA via the lone-paired electrons on nitrogen atom of PNPAA, is formed. This planar delocalization is a driving force to replace the self-association of PNPAA with inter-association to P4VP, and thus the inter-associative equilibrium constants (K_B) in PNPAA/P4VP at different temperatures are higher than those in poly(N-methyl methacrylamide)/P4VP (PNMAA/P4VP), even though the phenyl group is more steric hindered to prevent the formation of any kinds of hydrogen bonding. This planar delocalization is impossible in poly(N-cyclohexyl methacrylamide)/P4VP (PNCHAA/P4VP) blends, so the steric bulky cyclohexyl group hinders the formation of inter-association and self-association to obtain smaller K_A/K_B at different temperatures.

Moreover, based on the definition of the Bronsted-Lewis acid and base, the acidity of N–H and the basicity of the lone-paired electrons on nitrogen atom in aniline derivatives depend upon on the substitutions of aromatic ring. Introducing different electronegative substitution at *para*-position of aniline, the basicity of the lone-paired electrons on nitrogen atom and the acidity of N–H group can be affected through delocalization over the π system of aromatic ring. Comparing to aniline, if the *para*-substitution is an electron-donating group, such as methoxy group, the electron-donating group makes $-NH_2$ more electron-rich and electron-shielding, enhancing the basicity of the lone-paired electrons on nitrogen atom but reducing the acidity of the N–H bond with electron. In contrast, if the *para*-substitution is an electron-withdrawing group, such as bromo group, the electron-withdrawing group at *para*-position makes $-NH_2$ more electron-deficient and electron-deshielding, reducing the basicity of the lone-paired electrons on nitrogen atom in 4-methoxy but enhancing the acidity of the N–H bond. The basicity of lone-paired electrons on nitrogen atom and the acidity of NH_2 in aniline can be affected by *para*-substituent through the delocalization of the benzene ring, to speak nothing of the N–H bonding in their amide derivatives. In this work, a series of poly(*N*-phenyl methacrylamide) derivatives (Scheme 1) were designed to investigate the substituent-induced delocalization effects on self-associative hydrogen bonding and inter-associative hydrogen bonding by blending with poly(4-vinylpyridine) (P4VP). FTIR, DSC and solid-state NMR spectroscopy were used as tools to investigate the specific interaction.

2. Experimental

2.1. Materials

N-phenyl methacrylamide was purchased from TCI Chemical Company that was purified by column chromatography and recrystallization before its polymerization. Poly(4-vinyl pyridine) (P4VP) was purchased from Aldrich Chemical. The radical initiator azobisisobutyronitrile (AIBN) was recrystallized from ethyl alcohol prior to use. Dioxane was distilled under vacuum and then used as the solvent for the polymerization experiments performed in solution. Methacryloyl chloride, 4-bromoaniline and 4-methoxyaniline were used as received without further purification.

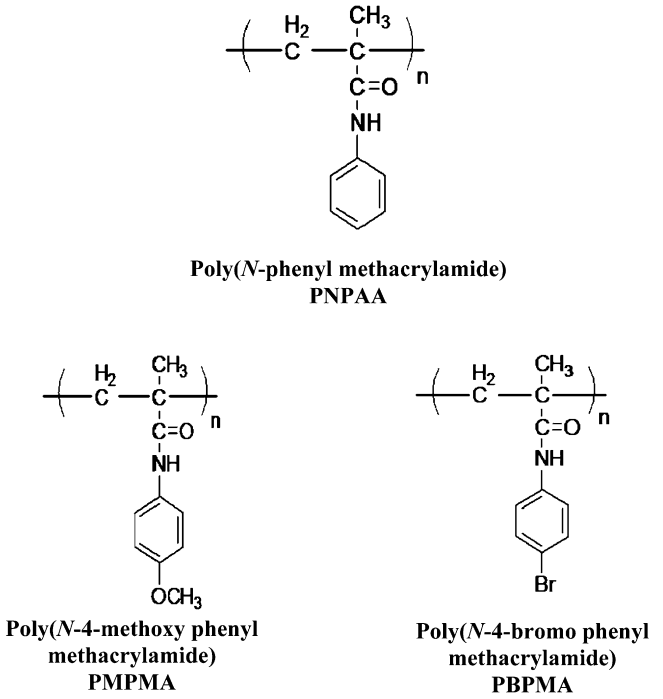

Scheme 1. The chemical structures of poly(*N*-phenyl methacrylamide), poly(*N*-4-methoxyphenyl methacrylamide) and poly(*N*-4-bromophenyl methacrylamide).

2.2. Synthesis

2.2.1. Synthesis of N-4-methoxyphenyl methacrylamide and N-4-bromophenyl methacrylamide

Two *N*-4-methoxyphenyl methacrylamide and *N*-4-bromophenyl methacrylamide were synthesized by adding different types of 4-methoxyaniline and 4-bromoaniline with methacroloyl chloride by the same reaction procedure. Methacryloyl chloride (0.05 mol, 5.82 mL) in 20 mL dried tetrahydrofuran (THF) in dropping funnel was slowly added to a stirred cold (0–5 °C) solution of 4-bromoaniline (0.5 mol) and triethylamine (0.06 mol, 8.31 mL; as catalyst) in 80 mL dried tetrahydrofuran in round bottom flask. The mixture was magnetically stirred for 24 h at room temperature. After removing the formed solid quaternary ammonium salt, the solution was transferred to a separating funnel, washed thoroughly with 5 wt% sodium hydroxide solution, dilute hydrochloric acid, and water, and then dried over anhydrous magnesium sulfate. On evaporation of the solvent, *N*-4-bromophenylmethacrylamide was obtained. ^{1}H NMR ($CDCl_3$, ppm) of *N*-4-bromophenyl methacrylamide: 2.0 (3H, methyl), 5.43 and 5.76 (2H, C═CH_2), 7.38 ~ 7.45 (4H, benzene), 7.88 (1H, NH). *N*-4-methoxyphenyl methacrylamide: 2.01 (3H, methyl), 3.76 (3H, OCH_3), 5.38 and 5.75 (2H, C═CH_2), 6.82 ~ 7.44 (4H, benzene), 7.74 (1H, NH).

2.2.2. Synthesis of poly(N-phenyl methacrylamide) (PNPAA), poly(N-4-methoxyphenyl methacrylamide) (PMPMA) and poly(N-4-bromophenyl methacrylamide) (PBPMA)

The degassed solutions of *N*-phenyl methacrylamide, *N*-4-methoxyphenyl methacrylamide and *N*-4-bromophenyl methacrylamide were carried out in dioxane at 70 °C under an argon atmosphere in a glass reaction flask equipped with a condenser. AIBN (1 wt% based on monomers) was employed as the initiator. The mixture was stirred for ca. 36 h before being poured into excess

hexane vigorous agitation to precipitate the product. The crude copolymer product was purified by redissolving it in dioxane and then adding this solution dropwisely into a large excess of hexane. This procedure was repeated several times and then the residual solvent of the final product was removed under vacuum at 70 °C for 1 day to yield pure white poly(*N*-phenyl methacrylamide), poly(*N*-4-methoxyphenyl methacrylamide) and poly(*N*-4-bromophenyl methacrylamide). The molecular weight of PNPAA, PMPMA, and PBPMA is 1600, 2000, 1800 g/mol, respectively.

2.3. Polymer blends

Blends of various binary PNPAA/P4VP, PMPMA/P4VP and PBPMA/P4VP blends were prepared by solution casting. N,N′-Dimethylformamide (DMF) solution containing 5 wt% polymer mixture was stirred for 2–3 days and then it was casting in a Teflon dish. The solution was left to evaporate at 100 °C in oven for 1 day, and the blend films were then dried at 120 °C in vacuum oven for 3 days to ensure no residual solvent.

2.4. Characterizations

The glass transition temperature of the copolymer was determined using a Du-Pont DSC-9000 DSC system. The sample was kept at 200 °C for 1 min and then cooled quickly to 30 °C from the melt of the first scan. The value of T_g was obtained as the inflection point of the jump heat capacity at a scan rate of 20 °C/min within the temperature range of 5–280 °C. Infrared spectra of the copolymer films were determined by using the conventional NaCl disk method. The DMF solution containing the blend was cast onto a NaCl disk. The film used in this study was thin enough to obey the Beer–Lambert law. FTIR measurements were performed on a Nicolet Avatar 320 FTIR spectrophotometer; 32 scans were collected at a spectral resolution of 1 cm^{-1} ^1H NMR spectra of these homopolymers were recorded on a Brucker ARX300 spectrometer using $CDCl_3$ as the solvent. High-resolution solid-state ^{13}C NMR spectroscopy experiments were performed at 25 °C using a Bruker DSX-400 spectrometer operating at a resonance frequency of 100.47 MHz. High-resolution solid-state ^{13}C NMR spectra were acquired using the cross-polarization (CP)/magic-angle spinning (MAS)/high-power dipolar decoupling (DD) technique, with a 90° pulse width of 3.9 μs, a pulse delay time of 3 s, an acquisition time of 30 ms, and 2048 scans. A magic-angle sample-spinning rate of 5.4 kHz was used to avoid absorption overlapping. The proton spin-lattice relaxation time in the rotating frame ($T_1\rho^H$) was determined indirectly via carbon observation using a 90 °C τ-spin lock pulse sequence prior to CP. The data acquisition was performed at delay times (τ) ranging from 0.1 to 10 ms with a contact time of 1.0 ms.

3. Results and discussion

3.1. Thermal analyses

Differential scanning calorimetry (DSC) is one of the convenient methods to observe thermal characteristic arising from different interactions in polymer blends. In addition, it is also useful to determine the miscibility in polymer blends. However, there exist many factors such as the nature of the solvent, composition, molecular weights, etc., affecting the formation of interpolymer interactions to change blends' miscibility. Besides these factors, we are particularly interested in the substituent-induced delocalization effects on the hydrogen-bonding behaviors. For this purpose, DMF is used as casting solvent, even though PNPAA/P4VP blends are miscible over the entire composition range casted from tetrachloroethane (TCE) in our previous publication [26]. Unfortunately, TCE is able to dissolve neither PMPMA nor PBPMA, and thus, DMF is used as the common solvent in this study.

Fig. 1 shows all the second run DSC thermalgrams of PNPAA/P4VP, PMPMA/P4VP and PBPMA/P4VP blends in various composition of weight ratio, and the T_gs are summarized in Table 1. In Fig. 1(a), PNPAA/P4VP blends are immiscible based on DSC analyses since most compositions of these blends show two glass transition temperatures, indicating less effective inter-associative hydrogen bonding between the amide units of PNPAA and the pyridine units of P4VP. The lower T_g in the range of 130–156 °C can be identified with the P4VP phase with PNPAA segments, and the higher T_g can be identified with the PNPAA phase with P4VP segments. More interestingly, the value of the lower-T_g phase in PNPAA/P4VP composition of 20/80 is even lower than that of pure P4VP. Such phenomenon had been discovered and demonstrated. Lu et al. reported that the values of T_g in miscible poly(styrene-*co*-vinylphenol dimethylsilano)/poly(*N*-vinyl-2-pyrrolidone) (PVP) blends containing 10 and 20 wt% of PVP were lower than that of the low-T_g

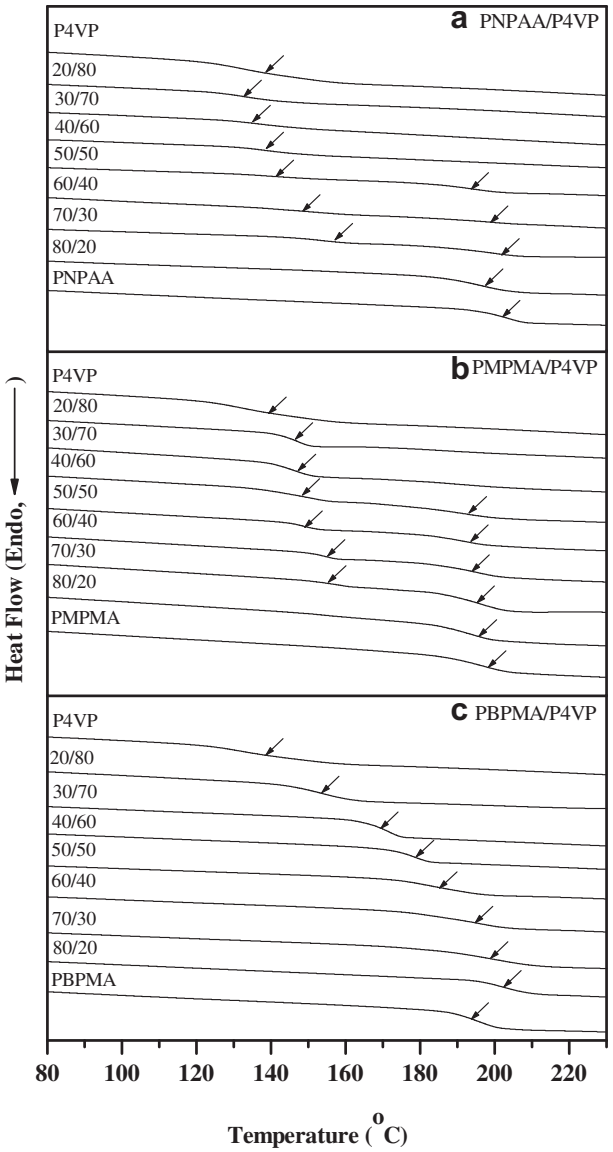

Fig. 1. DSC thermograms of (a) PNPAA/P4VP, (b) PMPMA/P4VP and (c) PBPMA/P4VP blend with different compositions.

Table 1
T_g behaviors of PNPAA/P4VP, PMPMA/P4VP and PBPMA/P4VP blend with different compositions.

Composition	T_g (°C)					
(amide/pyridine)	PNPAA/P4VP		PMPMA/P4VP		PBPMA/P4VP	
0/100			138			
20/80	132		146		155	
30/70	134		147		169	
40/60	138		149	193	178	
50/50	141	193	150	193	185	
60/40	149	199	155	194	195	
70/30	156	201	155	195	198	
80/20	196		198		202	
100/0	201		196		194	

component [34]. Huang et al. also certificated this phenomenon in their studies that in the poly(2,2,3,3,3-pentafluoropropyl methacrylate-*co*-4-vinylpyridine) (PFX, where X was denoted the mol% of 4-vinylpyridine unit in the copolymer)/poly(4-vinylphenol) blends, and the values of T_g were even lower than that of pure PF28 [35]. They suggested that the hydrogen-bonding interaction was not extensive and thus the chain segments were poorly packed, which give rise to a large increase in free volume and decreased T_g values. This explanation is reasonable for interpreting the abatement of T_g for the PNPAA/P4VP compositions of 20/80 and 30/70 comparing with the T_g of homo-P4VP in this study.

Fig. 1(b) shows the DSC thermograms of PMPMA/P4VP blends with different compositions. There are two T_gs in most compositions, indicating that there is not effective inter-associative hydrogen bonding between PMPMA and P4VP. The lower T_g in the range of 145–155 °C is assigned as P4VP domains and the higher T_g is assigned as PMPMA domains. The single T_g of the composition of 80/20 indicates that the few amount of P4VP contaminates PMPMA matrix; on the contrary, the single T_g of the compositions of 30/70 and 20/80 reveals that the few amount of PMPMA contaminates P4VP matrix, with higher value of T_g upon increasing PMPMA content. In addition, all the T_g of P4VP domains are higher than that of pure P4VP because of the hydrogen-bonding interaction is extensive and free-volume effect does not occur.

The DSC thermograms of PBPMA/P4VP blends are shown in Fig. 1(c). PBPMA is miscible with P4VP over the entire composition range with single glass transition, meaning that there is more effective inter-association between PBPMA and P4VP than that of PNPAA/P4VP and PMPMA/P4VP blends. Furthermore, the T_gs of miscible PBPMA/P4VP blends increases upon increasing the content of PBPMA. For miscible blends, T_g values can be described by several empirical equations [36–39] and the Kwei equation is usually employed for systems with specific interactions,

$$T_g = \frac{W_1 T_{g1} + kW_2 T_{g2}}{(W_1 + kW_2)} + qW_1 W_2 \quad (1)$$

where T_g is the glass transition temperature of the blend; T_{g1} and T_{g2} are those of the pure component; W_1 and W_2 are the weight fractions of the two components; k and q are adjustable parameters. The application of Eq. (1) on the T_g-composition data of the PBPMA/P4VP blends is best fitted by a curve (as shown in Fig. 2) with $k = 1$ and $q = 90$, where q is a parameter which is corresponding to the strength of hydrogen bonding in the blend and reflecting a balance between the breaking of the self-association and the forming of the inter-association hydrogen bonding. The positive q of 90 means a strong intermolecular interaction between PBPMA and P4VP. The reason for the immiscible behavior of PNPAA and PMPMA or miscible behavior of PBPMA with P4VP could be characterized by FTIR spectroscopy analyses.

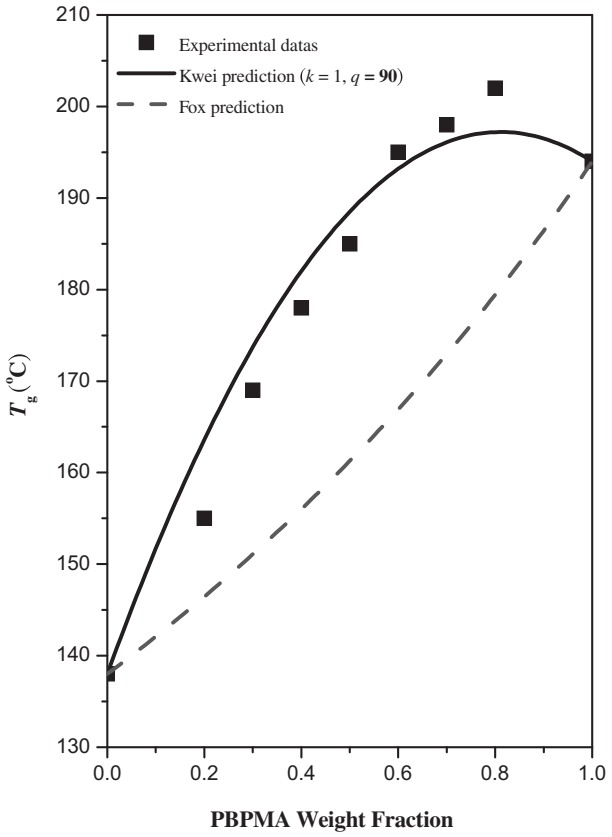

Fig. 2. Plot of T_g versus the composition of PBPMA/P4VP blends prepared from DMF. The curve is calculated using the Kwei equation with $k = 1$ and $q = 90$.

3.2. Strength of specific interaction, as determined by FTIR spectroscopy

3.2.1. Self-associative hydrogen bonding in PNPAA, PMPMA and PBPMA

FTIR spectroscopy has been proven to be a very powerful technique to detect the presence of self-association within a given molecule or inter-association between two chemically dissimilar molecules. Fig. 3 shows FTIR spectra recorded at room temperature for the three neat poly(*N*-phenyl methacrylamide) derivatives and scale-expanded FTIR spectra in the region of the carbonyl stretching vibration. In Fig. 3, PMPMA are observed for (1) the free carbonyl groups units at 1680 cm^{-1}, (2) the self-associated, hydrogen-bonded carbonyl groups at 1651 cm^{-1}. In PBPMA, the peak positions of free and hydrogen-bonded carbonyl groups are located at 1685 and 1655 cm^{-1}, respectively [40]. The peak positions of free and hydrogen-bonded carbonyl groups in PNPAA, which were obtained in our previous publication, are located at 1684 and 1659 cm^{-1}, respectively [26]. Here, we ignore the self-association hydrogen bonding with relatively weak aromatic—H-N bonding [33,41]. Zhang et al. pointed out that the difference in wavenumber ($\Delta\nu_H$) between the absorption bands of hydrogen-bonded and free functional groups can be used as a measure of the relative strength of hydrogen bonding [42], so the difference in wavenumber ($\Delta\nu_H$) between the absorption peaks of hydrogen-bonded and free carbonyl group in PNPAA is smaller than PMPMA and PBPMA, indicating that PNPAA, PMPMA and PBPMA possess different self-association hydrogen bonding strengths.

Moreover, according to the Painter–Coleman association model [40], the thermodynamics of polymer blends with hydrogen bonding can be written using the following scheme:

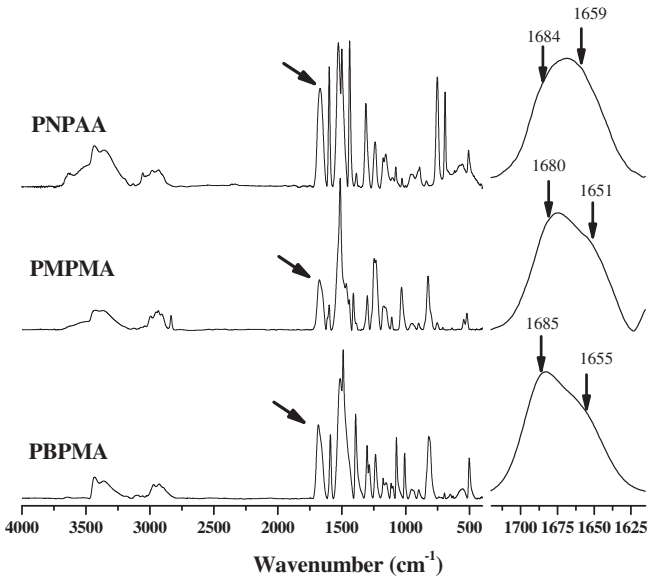

Fig. 3. FTIR spectra for three neat polymethacrylamides: PNPAA, PMPMA and PBPMA.

$$B_1 + B_1 \overset{K_2}{\rightleftharpoons} B_2$$
$$B_h + B_1 \overset{K_{h+1}}{\rightleftharpoons} B_{h+1}$$
$$B_h + A_1 \overset{K_A}{\rightleftharpoons} B_hA_1$$

Self-association

Inter-association

where B_1 represents amide-NH group, A_1 represents pyridine group, B_2 is the hydrogen-bonded dimmer formed between two amide groups, B_h is the hydrogen-bonded multimer, and B_hA_1 is the inter-associative hydrogen bonding. The change in the relative intensities of the free and hydrogen-bonded carbonyl bands vary systematically in favor of the former as temperature increasing, reflecting the decreasing fraction of hydrogen-bonded carbonyl groups present as a function of temperature. This is a measure of the enthalpy of hydrogen-bond formation. The methodology employed to determine the enthalpy of hydrogen-bond formation from infrared spectra has been discussed in detail on previous publication [40,41]. The equilibrium constant K_B of self-association of amide groups is related to the $f_F^{C=O}$ values through

$$K_B = \frac{1 - f_F^{C=O}}{\left[f_F^{C=O}\right]^2} \tag{2}$$

and the K_B at different temperatures could be calculated. Obviously, the equilibrium constants, and hence the stoichiometry of hydrogen boning, vary with temperature. This is simply described through the usual dependence on the enthalpy of hydrogen-bond formation:

$$K_B = K_B \exp\left[-\frac{\Delta h_B}{R}\left(\frac{1}{T} - \frac{1}{T^\circ}\right)\right] \tag{3}$$

where K_B is the value of the equilibrium constant determined at To K (usually 298 K), R is the universal gas constant, and Δh_B is the molar enthalpy of the formation of individual hydrogen bonds. Using Eq. (2) and Eq. (3), we can calculate the enthalpy of self-associative hydrogen-bond formation in PNPAA, PBPMA, except PMPMA. The lone-paired electrons on oxygen atom in ether group of PMPMA would be a hydrogen-bond acceptor, competing with the lone-paired electrons on oxygen atom in carbonyl group. However, the hydrogen-acceptor ability of the lone-paired electrons on ether oxygen is much smaller than that of carbonyl group in amide [42]. Thus, the small fraction of hydrogen-bonded methoxy group can be ignored, and this methodology still can be employed to calculate the enthalpy of self-associative hydrogen-bond formation in PMPMA.

The curve-fitting limits were set to 1560–1740 cm^{-1}, and the spectra were curve resolved into two bands using a lease-squares fitting procedure [40]. For PBPMA, Lorezian band shapes were fixed, the ν of the two bands were restricted to ranges of 1685 ± 1 cm^{-1} and 1655 ± 1 cm^{-1}, and $w_{1/2}$ was restricted to range 31.5 ± 1 cm^{-1} and 32.0 ± 1 cm^{-1}, respectively, for all the least-squares fits. Values of $a_{HB}/a_F = 1.2$ is employed to calculate the fraction of free and hydrogen-bonded carbonyl groups [39]. The calculations of K_B for the different temperatures are listed in the final column of Table 2. A van't Hoff plot of ln K_B versus the reciprocal of temperature is shown in Fig. 4, and we can obtain a value of 1.41 kcal/mol for the enthalpy Δh_B of hydrogen-bond formation from the slope of least-squares linear fit of the data in Table 2. The same methodology was employed to calculate the enthalpy of hydrogen-bond formation of PMPMA, with the value of 1.39 kcal/mol, and the Δh_B of PNPAA was obtained with value of 1.29 kcal/mol [33].

Table 2
Curve fitting of the fraction of free and hydrogen-bonded carbonyl group of PNPAA, PMPMA, and PBPMA.

Temp. (°C)	PNPAA			PMPMA			PBPMA		
	The fraction of free and hydrogen-bonded C=O[a]		K_B	The fraction of free and hydrogen-bonded C=O[b]		K_B	The fraction of free and hydrogen-bonded C=O		K_B
	f_F (%)	f_b (%)		f_F (%)	f_b (%)		f_F (%)	f_b (%)	
50	46.4	53.6	2.49	67.7	32.3	0.71	59.9	40.1	1.12
70	48.4	51.6	2.20	69.9	30.1	0.62	62.0	38.0	0.99
90	50.2	49.8	1.97	71.4	28.6	0.56	63.4	36.6	0.90
110	51.4	48.6	1.84	72.9	27.1	0.51	65.1	34.9	0.82
130	52.9	47.1	1.68	74.9	25.1	0.45	66.5	33.5	0.76
150	54.2	45.8	1.56	76.3	23.7	0.41	67.5	32.5	0.71
170	55.7	44.3	1.42	77.2	22.8	0.38	68.9	31.1	0.66
190	56.7	43.3	1.34	78.1	21.9	0.36	69.9	30.1	0.62
210	57.8	42.2	1.26	79.2	20.8	0.33	71.4	28.6	0.56

[a] The ν of the two bands were restricted to ranges of 1684 ± 1 cm^{-1} and 1659 ± 1 cm^{-1}, and the $w_{1/2}$ was restricted to range 27.0 ± 1 cm^{-1} and 34.0 ± 1 cm^{-1}, respectively.
[b] The ν of the two bands were restricted to ranges of 1680 ± 1 cm^{-1} and 1651 ± 1 cm^{-1}, and the $w_{1/2}$ was restricted to range 31.5 ± 1 cm^{-1} and 27.0 ± 1 cm^{-1}, respectively.

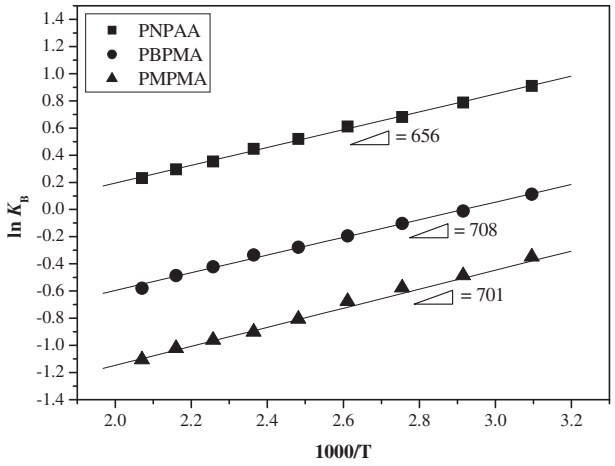

Fig. 4. The van't Hoff plots of ln K_B versus 1/T for PNPAA (■), PBPMA (●) and PMPMA (▲).

From the calculation of the enthalpy of self-associative formation in PNPAA, PMPMA and PBPMA, similar values of enthalpy are also obtained as the difference in wavenumber ($\Delta\nu_H$) between the absorption bands of hydrogen-bonded and free carbonyl groups; even though the equilibrium constants of PBPMA at each temperature is smaller than those of PNPAA. Bromine atom is a more steric bulky group than a hydrogen atom, the self-association between carbonyl and N—H group in PBPMA is much more difficult than the self-association in PNPAA, and thus equilibrium constants in PBPMA at different temperatures are smaller than those in PNPAA.

In Fig. 5, the scale-expanded spectra in the region of the carbonyl stretching vibration reveals that the peak positions of free and hydrogen-bonded carbonyl group shift because of *para*-substitutions. Electron-withdrawing group (—Br) makes the peaks of free and hydrogen-bonded carbonyl groups red-shift, and electron-donating group (—OCH_3) makes the peaks of free and hydrogen-bonded carbonyl groups blue-shift. However, the strength of self-association between carbonyl and N—H of amide group in three poly(*N*-phenyl methacrylamide) derivatives are comparable to each others. As shown in Fig. 5, through delocalization of benzene-π system, electron-donating group makes the amide group electron-rich, enhancing the hydrogen-bond acceptor ability of carbonyl group, but the proton on nitrogen in amide (N—H) is electron-shielded, with reduced hydrogen-bond donor ability. In contrast, electron-withdrawing group makes the amide group electron-deficient, reducing the hydrogen-bond acceptor ability of carbonyl group; but the proton on nitrogen in amide is electron-deshielded, with enhanced hydrogen-bond donor ability. Two factors are offset by each other, so that the values of enthalpy of self-association in poly(*N*-phenyl methacrylamide) with different inductive substitution at *para* position of benzene ring are not affected by the substituent-induced delocalization.

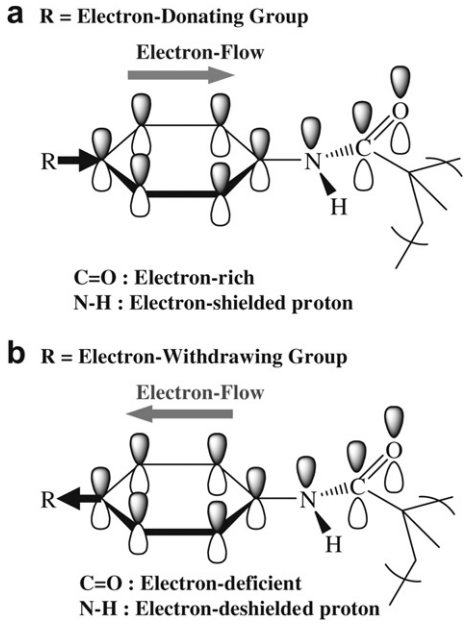

Fig. 5. The electron-flow pathway induced by *para*-substitution in poly(*N*-phenyl methacrylamide).

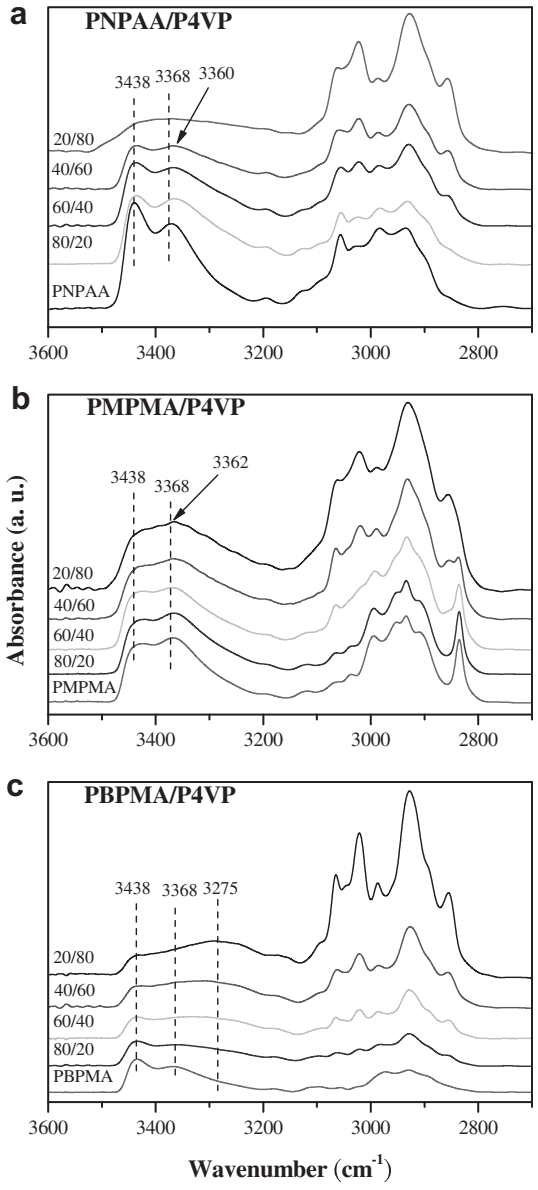

Fig. 6. FTIR spectra at 120 °C for (a) PNPAA/P4VP blends, (b) PMPMA/P4VP blends, and (c) PBPMA/P4VP blends.

3.2.2. Inter-associative hydrogen bonding in PNPAA/P4VP, PMPMA/P4VP and PBPMA/P4VP blends

Fig. 6 gives FTIR spectra of the N–H stretching region for PNPAA/P4VP, PMPMA/P4VP and PBPMA/P4VP blends at 120 °C, because P4VP and polymethacrylamides absorb moisture from air very easily. Clearly, pure PNPAA, PMPMA, and PBPMA all show the two absorption band corresponding to free amide N–H group at ca. 3438 cm^{-1} and hydrogen-bonding amide group at ca. 3368 cm^{-1}. The intensity of free amide N–H group was decreased and the hydrogen-bonding amide group from shifts to a lower wavenumber with the increase of P4VP contents in all three binary blend systems. This result reflects a new distribution of hydrogen-bonding formation resulting from the competition between amide–amide and amide–pyridine interactions. Zhang et al. pointed out that the difference in wavenumber ($\Delta\nu_H$) between the absorption bands of hydrogen-bonded and free phenolic groups could be used as a measure of the relative strength of hydrogen bonding [42]. The wavenumber of amide–pyridine hydrogen bond was located at 3360 cm^{-1}, 3362 cm^{-1}, and 3275 cm^{-1} as shown in Fig. 6 for PNPAA/P4VP, PMPMA/P4VP, PBPMA/P4VP blends, respectively, indicating that the fraction of hydrogen bonding in PBPMA/P4VP blends is higher than those in PNPAA/P4VP and PMPMA/P4VP blends. From the DSC thermograms, PBPMA/P4VP blends are homogeneous over entire composition range, while most compositions of PNPAA/P4VP and PMPMA/P4VP blends are heterogeneous, indicating that the possession of higher inter-associative strength than self-associative strength does not guarantee to obtain a miscible polymer blend. Actually, much larger K_A than K_B does ensure a miscible blend [1,43,44]. As shown in Fig. 6, the intensity of inter-associative hydrogen-bonded N–H stretching with P4VP in PBPMA/P4VP blends is obviously higher than that in PNPAA/P4VP and PMPMA/P4VP blends, meaning a larger K_A/K_B ratio in PBPMA/P4VP blends.

The relative strength of self-associative hydrogen-bond formation in PNPAA, PMPMA and PBPMA are comparable to each other, because the substituent-induced delocalization effects on N–H and C=O is offset by each other as the description above. Nevertheless, the relative strength of inter-associative hydrogen-bond formation and the further miscibility in PNPAA/P4VP, PMPMA/P4VP and PBPMA/P4VP blends are different from each others, indicating that the hydrogen-bond donor ability of N–H in amide group is the factor affected by substituent-induced delocalization. When a pyridine group in P4VP forms a hydrogen bond with the N–H group in amide (see in Fig. 7), a planar delocalization is constructed by the aromatic-π system of pyridine in P4VP, the aromatic-π system and the carbonyl-π system of amide group in poly(*N*-phenyl methacrylamide)s via the lone-paired electrons on nitrogen atom [26]. The *para*-substitution can affect the inter-associative hydrogen bonding between amide and pyridine through this planar delocalization. Electron-donating group in PMPMA makes the amide group electron-rich, so the proton on nitrogen in amide is electron-shielded, with lower hydrogen-bond donor ability than that of PNPAA. In contrast, electron-withdrawing group in PBPMA makes the amide group electron-deficient, so the proton on nitrogen in amide is electron-deshielded, with higher hydrogen-bond donor ability than that of PNPAA.

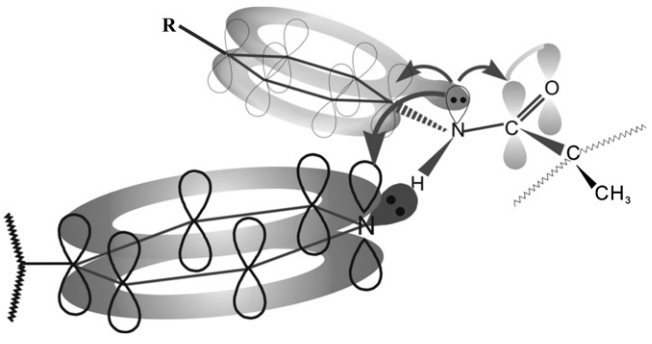

Fig. 7. The planar delocalization over carbonyl, phenyl aromatic and pyridine-aromatic π systems via the lone-paired electrons on nitrogen atom constructed by inter-associative hydrogen bond between poly(*N*-phenyl methacrylamide) derivatives and P4VP units.

3.3. ^{13}C CP/MAS solid-state NMR spectroscopic analyses

In addition to FTIR, evidences on interactions in the blends can also be obtained from solid-state NMR spectroscopy as demonstrated by changes in chemical shift and/or line shape. Fig. 8 shows the selected ^{13}C CP/MAS spectra of PNPAA/P4VP, PMPMA/P4VP and PBPMA/P4VP at the composition of 20/80, comparing with that of pure PNPAA and pure P4VP. Five peaks are also observed for pure P4VP where the peak at δ = 123.9 ppm and corresponds to the pyridine carbon atom. Clearly, the pyridine carbons shift in PBPMA/P4VP-20/80 downfields about 3.8 ppm significantly also indicating that the hydrogen-bonding interaction between the amide group of PBPMA and the pyridine group of P4VP. The pyridine carbons shift in PNPAA/P4VP-20/80 and PMPMA/P4VP-20/80 downfield about 3.2 and 3.0 ppm, respectively, and this finding is consistent with the results of our FTIR spectroscopic analysis.

Solid-state NMR spectroscopy is often used to better understand the phase behavior and interactions within polymer blends [45–48]. As discussion above, the DSC analyses reveal that phase separation occurred in PNPAA/P4VP and PMPMA/P4VP blends in certain compositions. However, it is must be kept in mind that the compositions with single transition temperature may be heterogeneous instead of homogeneous, because the dimension of phase separation may be too small to be detected by DSC analysis. One of the methodology employed to analyze the dimension of phase separation smaller than 20 nm is a measurement of the spin-lattice relaxation time in the rotating frame ($T_1\rho^H$) [34]. The $T_1\rho^H$ value of the blends was measured through the delayed-contact ^{13}C/MAS experiments. The $T_1\rho^H$ values are calculated from Eq. (4):

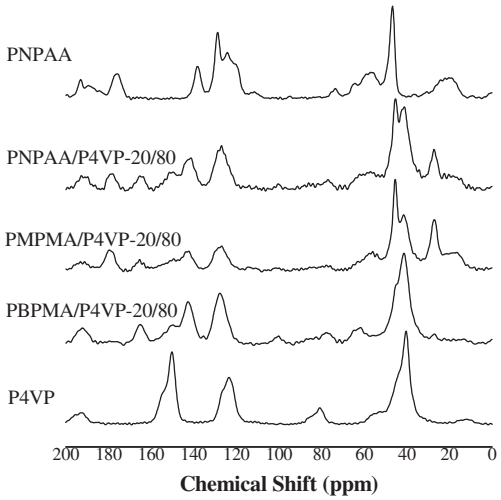

Fig. 8. ^{13}C CP/MAS spectra of PNPAA/P4VP, PMPMA/P4VP and PBPMA/P4VP at the composition of 20/80.

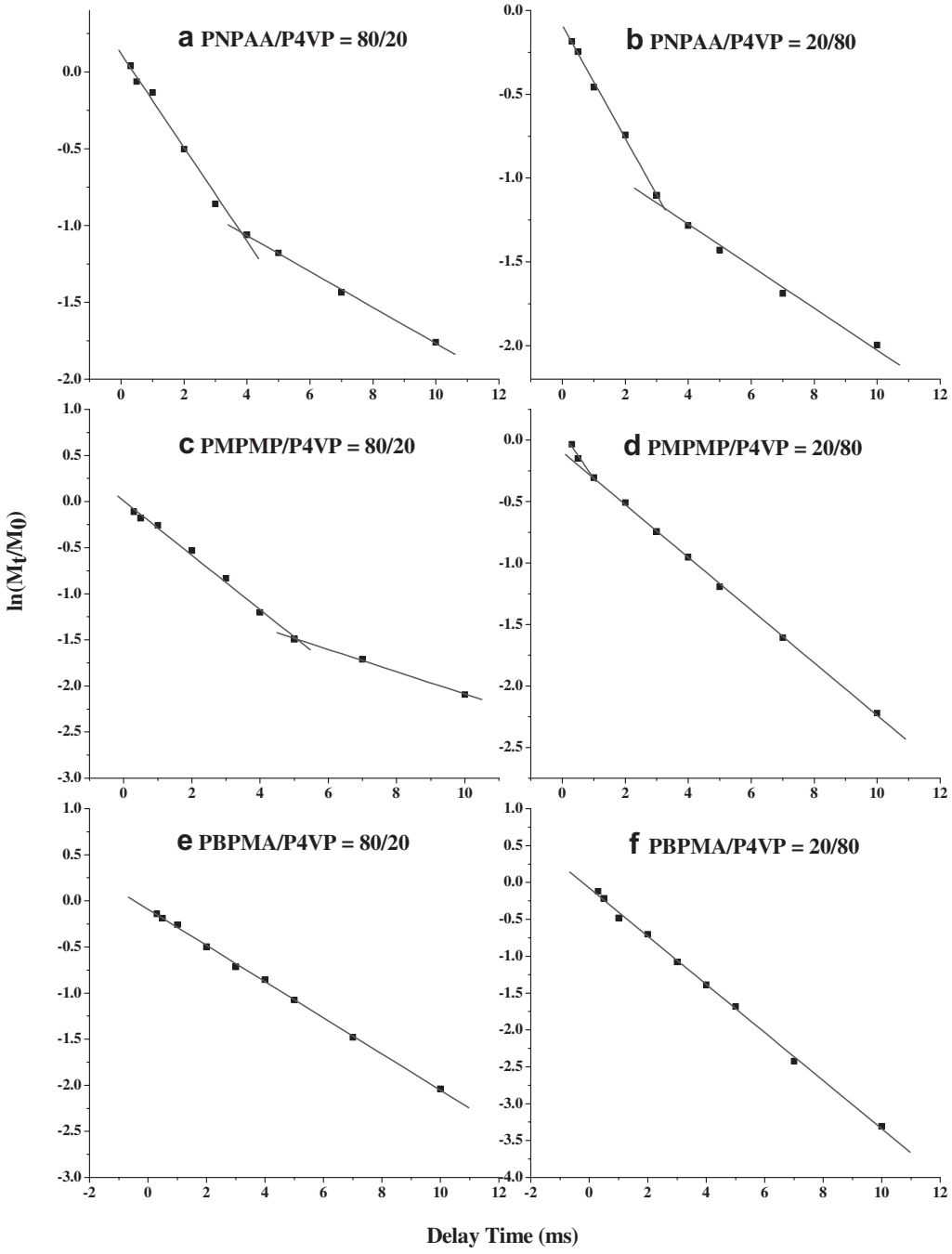

Fig. 9. Logarithmic plots of magnetization intensities of 176 ppm versus delay time for PPMA/P4VP blends (a) 80/20 and (b) 20/80; for PMPMA/P4VP blends (c) 80/20 and (d) 20/80; for PBPMA/P4VP blends (e) 80/20 and (f) 20/80.

$$\ln(M_\tau/M_o) = -\tau/T_1\rho^H \quad (4)$$

where τ is the delay time used in the experiment, M_0 and M_τ are the intensities of the peaks initially and at time τ, respectively. Fig. 9 shows the plots of ln (M_τ/M_0) against τ. We estimated the homogeneities of these polymer blends through quantitative analyses based on the main-chain-methylene carbon atom's resonance in poly(methacrylamide) at 46 ppm. Two exponential decays in $T_1\rho^H$ for PNPAA/P4VP = 80/20, 20/80 and PMPMA/P4VP = 80/20, 20/80 can be observed in Fig. 9 and Table 3, indicating that two domains possessing distinct mobility are present in PNPAA/P4VP and PMPMA/P4VP blends for entire compositions, except PNPAA blends and PMPMA blends with compositions of 80/20 and 20/80 appearing single T_g in DSC analyses. This result is consistent with the assumption that the phase separation may not be measured in DSC. In contrast, single-exponential decays in $T_1\rho^H$ for PBPMA/P4VP blends are obtained in Fig. 9, meaning that both

Table 3
Value of relaxation time ($T_1\rho^H$) for PNPAA/P4VP, PMPMA/P4VP and PBPMA/P4VP blends.

Composition amide/pyridine	$T_1\rho^H$(ms)		
	PNPAA/P4VP	PMPMA/P4VP	PBPMA/P4VP
100/0	4.14	4.71	5.36
80/20	3.33/9.09	3.25/8.33	5.16
20/80	3.03/7.69	2.75/4.76	3.12

PBPMA blends are homogeneous on the scale at which spin-diffusion occurs within the time $T_1\rho^H$. Thus the interaction between PBPMA and P4VP is the largest among these three binary blends. These conclusions are also consistent with the results of infrared and DSC analyses.

4. Conclusions

In this literature, we have successfully synthesized poly(*N*-phenyl methacrylamide) (PNPAA), poly(*N*-4-methoxyphenyl methacrylamide) (PMPMA) and poly(*N*-4-bromophenyl methacrylamide) (PBPMA), to investigate the substituent inductive effect on self-association and inter-associative interaction with P4VP. Variable-temperature FTIR spectra of three homopolymers provided evidences that the fraction of hydrogen-bonded carbonyl groups decreases upon elevating temperatures because of destroying the self-association. Through the least-square curve-fitting procedure and the van't Hoff plots of ln K_B versus $1/T$, the enthalpy of self-associative bond formation can be calculated. From the results of the calculation and the difference in wavenumber between free and hydrogen-bonded carbonyl group in three homopolymers, the substituent induction affect the enthalpy of self-associative hydrogen-bond formation slightly. However, in their binary blends with P4VP, the difference in wavenumber ($\Delta\nu_H$) between free and hydrogen-bonded N–H group in PBPMA/P4VP blends is obviously larger than those in PBNPAA/P4VP and PMPMA/P4VP blends, indicating that electron-withdrawing substituent induction enhance the strength of inter-association in polymethacrylamides/P4VP blends. This result is caused by that the substituent-induced electron resonance (i.e. bromo group of PBPMA and methoxy group of PMPMA) through planar delocalization. The inductive substitution at *para* position of benzene, regardless of electron-donating or electron-withdrawing group, can affect the electron delocalization over the benzene ring and the carbonyl-π system via the lone-paired electrons on nitrogen atom, changing the electron-cloud density of N–H or C=O groups and the strength of self-association and inter-association with P4VP. Moreover, comparing to electron-donating group ($-OCH_3$), electron-withdrawing group ($-Br$) can strengthening inter-associative hydrogen-bonding interactions. Furthermore, the proton spin-lattice relaxation time in the rotating frame ($T_1\rho^H$) employed by ^{13}C solid-state NMR spectroscopy indicates that the microphase separation occurs in PNPAA/P4VP and PMPMA/P4VP blends, but PBPMA/P4VP blends are homogeneous on the scale at which spin-diffusion occurs within the time $T_1\rho^H$, indicating that there is more effective specific interaction between PBPMA and P4VP.

Acknowledgment

This work was supported financially by the National Science Council of the R.O.C. under Contract No. NSC 97-2221-E-110-013-MY3 and NSC 98-2221-E-110-006.

References

[1] Coleman MM, Painter PC. Prog Polym Sci 1995;20:1.
[2] Kuo SW. J Polym Res 2008;15:459.
[3] Yang Z, Han CD. Macromolecules 2008;41:2104.
[4] Kuo SW, Chang FC. Macromolecules 2001;34:5224.
[5] De Mefathi MV. Frechet JMJ Polym 1988;29:477.
[6] Ten-Brinke G, Ruokolaine J, Ikkala O. Adv Polym Sci 2007;207:113.
[7] Cowie JMG, Reid VMC, McEwen IJK. Polym 1990;31:486.
[8] Chen WC, Kuo SW, Lu CH, Chang FC. Macromolecules 2009;42:3580.
[9] Motzer HR, Painter PC, Coleman MM. Macromolecules 2001;34:8390.
[10] Kuo SW, Hsu CH. Polym Inter 2010;59:998.
[11] Liu S, Chan CM, Weng LT, Jiang M. J Polym Sci B Polym Phys 2005;43:1924.
[12] Kuo SW, Tsai ST. Macromolecules 2009;42:4701.
[13] Lin IH, Kuo SW, Chang FC. Polym 2009;50:5276.
[14] Zhao JQ, Pearce EM, Kwei TK. Macromolecules 1997;30:7119.
[15] Chen WC, Kuo SW, Jeng US, Chang FC. Macromolecules 2008;41:1401.
[16] Kuo SW. Polym 2008;49:4420.
[17] Chen WC, Kuo SW, Chang FC. Polym 2011;51:4176.
[18] Wang C, Wang TM, Pei XQ, Wang QH. Polym 2009;50:5268.
[19] Kuo SW, Liu WC. J Appl Polym Sci 2011;119:300.
[20] Kuo SW, Lin CL, Chang FC. Macromolecules 2002;35:278.
[21] Kuo SW. J Appl Polym Sci 2009;114:116.
[22] Lee SC, Woo EM. J Polym Sci Polym Phys 2002;40:747.
[23] Kuo SW, Chan SC, Wu HD, Chang FC. Macromolecules 2005;38:4729.
[24] Coleman MM, Pehlert GJ, Painter PC. Macromolecules 1996;29:6820.
[25] Painter PC, Veytsman B, Kumer S, Shenoy S, Graf JF, Xu Y, et al. Macromolecules 1997;30:932.
[26] Painter PC, Park Y, Coleman M. J Appl Polym Sci 1998;70:1273.
[27] He Y, Zhu B, Inoue Y. Prog Polym Sci 2004;29:1021.
[28] Painter PC, Park Y, Coleman MM. Macromolecules 1988;21:66.
[29] Thibault RJ, Hotchkiss PJ, Gray M, Rotello VM. J Am Chem Soc 2003;125:11249.
[30] Cooke G, Rotello VM. Chem Soc Rev 2002;31:275.
[31] Woodford JN. J Phys Chem A 2007;111:8519.
[32] Jeffrey GA. An introduction to hydrogen bonding. New York: Oxford University Press; 1997. Ch.6.
[33] Lin CT, Kuo SW, Lo JC, Chang FC. J Phys Chem B 2010;114:1603.
[34] Lu S, Pearce EM, Kwei TK. Polym 1995;36:2435.
[35] Huang HL, Goh SH, Wee ATS. Polym 2002;43:2861.
[36] Chang M, Myerson S, Kwei TK. J Appl Polym Sci 1997;66:279.
[37] Dong J, Ozaki Y, Nakashima K. Macromolecules 1997;30:1111.
[38] Chalapathi VV, Ramiah KV. Curr Sci 1968;16:453.
[39] Zhang X, Takegoshi K, Hikichi K. Macromolecules 1992;25:2336.
[40] Coleman MM, Graf JF, Painter PC. Specific interactions and the miscibility of polymer blends. Lancaster: PA: Technomic Publishing; 1991.
[41] Choperena A, Painter P. Macromolecules 2009;42:6159.
[42] Zhang SH, Jin X, Painter PC, Runt J. Polym 2004;45:3933.
[43] Kuo SW, Chan SC, Chang FC. Macromolecules 2003;36:6653.
[44] Chen SC, Kuo SW, Jeng US, Chang FC. Macromolecules 2010;43:1083.
[45] Hill DJT, Whittaker AK, Wong KW. Macromolecules 1999;32:5285.
[46] Lau C, Mi Y. Polym 2001;43:823.
[47] Kuo SW, Chang FC. Macromolecules 2001;34:4089.
[48] Kuo SW, Tung PH, Chang FC. Macromolecules 2006;39:9388.